ISSN: 0067-2904

Spectral Analysis of the Effects of Variation in Electrodes' Area for Dielectric Barrier Discharge Actuator

Aseel Kamel Abd , Qusay Adnan Abbas
Department of Physics, College of Science, University of Baghdad, Baghdad, Iraq

Received: 23/4/2022 Accepted: 1/8/2022 Published: 30/4/2023

Abstract

In this work, one configuration was used to study the electrical discharge resulting from the dielectric barrier. This configuration consists of a sheet of epoxy/Al composite with dimensions of 75 mm in length, 25 mm in width, and 3 mm in thickness. This panel is located at the center of the electrodes, so that the distance between each of the electrodes and the plate is 2 mm and plasma is generated at these distances. The relationship between voltage and current with changing the frequency of the equipment as well as changing the area of exposure to the upper electrode or changing its length has been studied. The length of the top electrode varies at 0, 10, 20, 30, and 40 mm from the center of the electrodes producing exposure areas of 1875, 1625, 1375, 1125, 875, and 625 mm^2, respectively. Two frequencies of 8 and 9 kHz were applied in this work. The results showed that the discharge current increases linearly with the applied input voltage and with the decrease of the exposure of the upper electrode. Then, the current increases with the stability of the voltage in varying proportions depending on the exposure area and frequency. The plasma generated from this modulation was diagnosed with the exposure area and the fitted frequency. Electron temperature and electron density are calculated using the optical emission spectroscopy technique by Boltzmann and Lorenz, respectively. It can be seen that the temperature, electron density, and plasma frequency increase with the decrease of the exposure area, while the Debye length shows the opposite behavior and this is clear in this formation and high effectiveness at Diagnosis and Reason This formation will be adopted in the surface treatment of the aluminum epoxy compound.

Keywords: Dielectric Barrier Discharge actuator, surface configuration, I-V Characterization, diagnostic plasma, Boltzmann plot method

التحليل الطيفي لتأثيرات التغير في منطقة الأقطاب الكهربائية لمشغل تفريغ الحاجز العازل

أسيل كامل عبد ، قصي عدنان عباس
قسم الفيزياء, كلية العلوم, جامعة بغداد, بغداد, العراق

الخلاصة

تم استخدام تشكيل واحد لدراسة التفريغ الكهربائي الناتج من الحاجز العازل في هذا العمل. يتكون هذا التشكيل من لوح من مركب الايبوكسي المنيوم بابعاد 75 ملمتر الطول و25 ملمتر العرض و3 ملمتر السمك ويقع هذا اللوح بمركز الاقطاب الكهربائية بحث تكون المسافة بين كل من الاقطاب واللوح 2ملمتر وتتولد

*Email: waleed.yaseen@sc.uobaghdad.edu.iq

البلازما في هذه المسافات. تم دراسة العلاقة بين الفولتية والتيار مع تغير تردد المجهز وكذلك تغير مساحة التعرض للقطب العلوي او تغيير طوله. يتغير طول القطب العلوي عند 0 و 10 و 20 و 30 و 40 ملمتر من مركز الأقطاب الكهربائية التي تنتج مناطق تعرض 1875 و 1625 و 1375 و 1125 و 875 و 625 ملم على التوالي. تم تطبيق ترددين 8 و 9 كيلو هرتز في هذا العمل. أظهرت النتائج أن تيار التفريغ يزداد خطيًا مع جهد الدخل المطبق وأيضًا مع تناقص في مساحة التعرض للقطب العلوي وبعد ذلك يزداد التيار مع ثبوت الفولتية بنسب متفاوتة تعتمد على مساحة التعرض والتردد. تم تشخيص البلازما المتولدة من هذا التشكيل مع مساحة التعرض وتردد المجهز. درجة حرارة الإلكترون، والكثافة الالكترونية يتم حسابها باستخد م تقنية التحليل الطيفي للانبعاثات الضوئية بطريقة بولتزمان وطريقة ولورنز على التوالي ويمكن ملاحظة زيادة درجة الحرارة وكثافة الإلكترون وتردد البلازما مع انخفاض مساحة التعرض بينما طول ديباي يظهر السلوك المعاكس وهذا ماظهر واضحا في هذا التشكيل واضهر فعالية عالية عند التشخيص ولها السبب سيتم اعتماد هذا التشكيل في المعالجة السطحية لمركب ايبوكسي المنيوم.

1. Introduction

Using Dielectric Barrier Discharge (DBD) as a plasma generator has been used in a variety of research and development projects. DBD is a type of low-temperature plasma that can be used in different applications, including the environment, DBD actuator, ozone generators, and more [1]. Brandenburg studied the plasmas generated in configurations with an insulating (dielectric) material between the electrodes which is responsible for a self-pulsing operation [2]. Kanazawa et al. [3], Massines et al. [4], and Roth et al [5]. successfully generated relatively large volume, non-equilibrium, diffused atmospheric pressure plasma using the Dielectric Barrier Discharge (DBD) technique. These researchers mostly employed a planar shape electrode and sinusoidal voltages in kV at a frequency of 10 kHz [6]. Researchers have shown a lot of interest in plasma active flow control using atmospheric surface discharges. Its desirable properties, such as simple configuration and real-time control, have made it promising and unique for its utilization in the domain of flow controller, such as reducing drag force energy loss and acoustic noise, improving airfoil lift, and increasing heat transfer rate, among others [7]. To generate plasma at ordinary pressure with high voltage, the electrodes' gap of discharge should be in a range of (0.1–10) mm [8].

Surface dielectric barrier discharge (SDBD) uses a high-voltage alternating current (AC), in the order of kilo volts, to provide a periodic alternating potential difference (and thus electric field) between the two electrodes. When the field strength is strong enough, the air is ionized and creates non-thermal plasma, while the dielectric barrier allows a charge build-up that limits the discharge and prevents arcing between the electrodes. The electric field exerts a Coulomb force on the plasma's ions, which is then transferred to the surrounding air via ion-neutral collisions [9] [10]. The corona discharge and the dielectric barrier discharge DBD are two extensively used methods for producing non-thermal plasma at atmospheric pressure [11]. Industrial ozone generation, surface modification of polymers, plasma chemical vapor deposition, excitation of CO_2 lasers, excimer lamps, and, most recently, large-area flat plasma display panels are all important applications for this type of plasma. DBDs have been studied for a biological purge of medical devices, air flows, and tissues since the 1990s. They are also employed in novel analytical detection devices or as sources of electric wind in aerodynamic control systems [12] [13]. Optical Emission Spectrometry (OES), which is the spectral examination of the light originating from plasma, is a significant and extensively used plasma diagnosis method, especially for atmospheric pressure plasma sources. Several of the most significant plasma parameters, such as electron density, electron temperature, electric field, and so on, are obtained using OES [14].

This work used Epoxy/Al composite as the dielectric material (of dimensions 60 mm length, 20 mm width, and 3 mm thickness) positioned in the middle distance between the two electrodes with a variable exposure area for the upper electrode.

2. Theoretical Description of Plasma Parameters

The OES technique is much used in the diagnosis of laboratory plasma, such as discharge plasma, radio frequency inductively coupled plasma, laser-induced plasma, and DBD plasma [15]. The OES technique used in this study aimed to identify the properties of DBD plasma: electrons temperature (T_e) and electron density(n_e) [16]. The emitted radiation from plasma give more details about plasma properties, and (OES) is the best technique for assessing plasma parameters and predicting plasma radiation emission [17]. The Ions and electrons' average random kinetic energy is related to their temperature. Maxwell distribution determines the distribution of velocities for each type of particles in thermal equilibrium [18]. The two intensity ratio technique, Boltzmann plot, Saha-Boltzmann equation, and Doppler broadening are the four most often used methods for calculating temperature. [19].

Given that the population densities of the lines in the higher level are in Local Thermodynamic Equilibrium (LTE), the simplest technique for determining the temperature is to use the intensity ratio of two spectral lines. Keeping in mind that the temperature acquired with this method is the excitation temperature; at LTE, the temperature becomes electron temperature. The optically narrow spectral line's intensity is computed as follows [20].

$$I_{ij} = \frac{hcA_{ij}g_j n}{\lambda_{ij}U(T)} e^{\left(\frac{E_j}{kT}\right)} \quad (1)$$

The intensity and wavelength of the transition from i to j, respectively, are I_{ij} and λ_{ij}. Planck constant is h, speed of light is c, number density of emitting species is n, partition function is U (T), the transition probability between levels i and j is A_{ij}, Boltzmann constant is k, excitation temperature is T, and the top energy level is E_j in eV. Rearranging Eq. (1) gives:

$$\left(\frac{\lambda_{ji}I_{ji}}{hcA_{ji}g_j}\right) = \frac{n}{U(T)} e^{\frac{E_j}{kT}} \quad (2)$$

When the natural logarithm is applied to both sides of Eq. (2), the result is:

$$\ln\left(\frac{\lambda_{ji}I_{ji}}{hcA_{ji}g_j}\right) = -\frac{1}{kT}(E_j) + \left(\ln\frac{N}{U(T)}\right) \quad (3)$$

Eq. (3) produces a linear relationship when graphing ((λ_{ji} I_{ji})(hcA_{ji} g_j)) vs E_j, and the slope of the curve can be used to calculate T_e. Also, the Boltzmann plot requires peaks of the same atomic type and ionization stage. The Boltzmann plot has an advantage over the ratio technique in that optically thick lines large variances in data points in straight line fitting can be distinguished [20]. The Saha-Boltzmann equation and the Stark broadening relationship are two approaches for calculating electron density, which are covered in this section. The electric field of ions and electrons causes Stark broadening, resulting in spectral broadening with the FWHM as described by the equation [15]:

$$\Delta\lambda_{1/2} = 2\omega\left(\frac{n_e}{10^{16}}\right) \quad (4)$$

Where: n_e is the electron density, ω is the electron impact parameter, and $\Delta\lambda_{1/2}$ is the FWHM of the Stark broadened spectral peak.

The characteristics of nitrogen can be determined using information from optical emission spectroscopy and National Institute of Standards and Technology (NIST) Database [21].

A feature of plasma is its ability to shield out electric potentials that are applied to it. The response of charged particles to restrict the influence of local electric fields is known as Debye shielding, and it is this shielding that causes the plasma to be quasi-neutral. The Debye length, commonly known as a distance λ_D, is defined as:

$$\lambda_D = \left(\frac{\varepsilon_o kT_e}{n_e e^2}\right)^{\frac{1}{2}} \quad (5)$$

Where: ε_o is the permittivity of free space, and e is the electron charge.
The number of particles in the Debye sphere (N_D) represents second criterion for plasma existence $N_D>>1$; it depends on n_e and λ_D, as shown in the following equation [22] [23]:

$$N_D = \frac{4\pi}{3} n_e \lambda_D^3 \quad (6)$$

Electric fields are produced when electrons in the plasma are displaced from a uniform background of ions, the electrons get back to their original places by way pull, and the neutrality of plasma is restored. The plasma frequency is a characteristic frequency occurring when the electrons exceed and oscillate around their equilibrium positions and because of their inertia:

$$\omega_p = \left(\frac{ne^2}{\varepsilon_o m}\right)^{\frac{1}{2}} \quad (7)$$

Where: ω_p is the plasma frequency, and m is the electron mass. Numerically, one can use the approximate formula:

$$f_p = \frac{\omega_p}{2\pi} = 9\sqrt{n_e} \quad (8)$$

The natural plasma frequency is denoted by f_p. One of the essential properties of plasma is frequency, which is solely dependent on the plasma density, as can be seen from Eq. 8. The frequency of plasma is normally very elevated due to the small mass of electrons m_e [24].

3. Experimental Specifics

A schematic diagram of the DBD actuator is shown in Figure 1. An AC power supply was used to produce a high voltage of 20 kV (peak to peak) at a frequency of (1-50) kHz. This AC high voltage was applied to the upper electrode with the lower electrode grounded. An epoxy mixed with aluminum was used as a dielectric material between the electrodes.

The distance between the electrodes and the dielectric barrier was 2 mm. The electrode gap was filled with air at atmospheric pressure. The electrodes of dimension 75mm length, 25mm, width and 3mm thickness were used. The upper electrode to the center of the electrodes distance was changed (0, 10, 20, 30, and 40) mm corresponding to a change of the exposure area of (1875, 1625, 1375, 1125, and 875) mm^2, respectively.

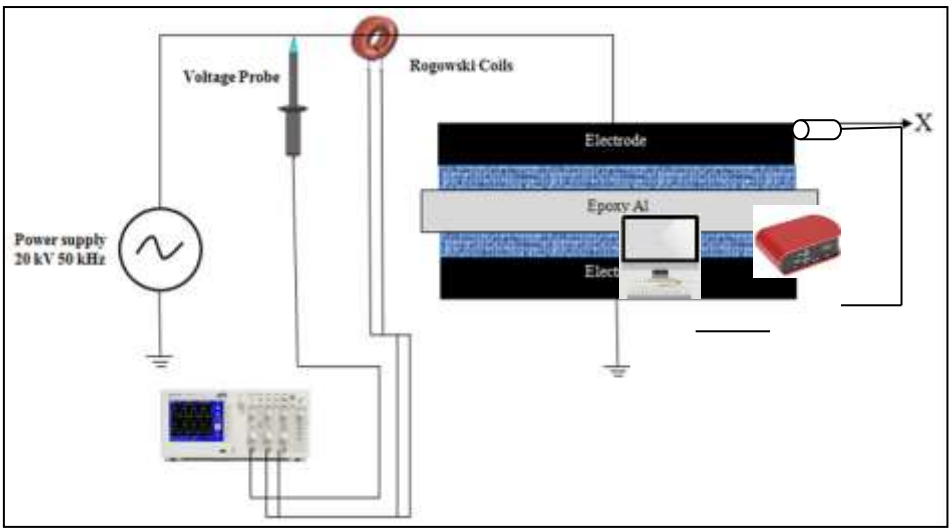

Figure 1: Experimental set-up of DBD actuator

The plasma is generated between the higher electrode and the dielectric and the lower electrode and the dielectric. The experiments were done at room temperature under

atmospheric pressure. The high voltage applied on the electrodes was measured using 40 kV, 50kHz AC probe. Rogowski coil was utilized to measure the circuit current. The digital oscilloscope (UNI-T UTD2000 100 MHz) using to stored voltage applied on the electrodes and the total current. From the measured voltage and current, the I-V characteristic scan be plotted. In this study, important information such as capacitance, phase difference between current and voltage and power density of the plasma can be determined from the measured voltage and current parameters. To describe the plasma and to calculate the electron temperature and density, the OES technique was applied. A Thorlabs Charge-Coupled Device (CCD) Spectrometer with a maximum resolution of 1.5 nm was used to collect OES data. To ensure higher efficiency of the results, an optical fiber was positioned between the two electrodes at a distance of 1.0 mm from the edge of the anode to acquire spectra.

4. Results and Discussion

4.1 I-V Characteristics

The upper electrode was displaced from the center of the electrodes by a distance 0, 10, 20, 30, and 40 mm and two frequencies 8 and 9 kHz is applied in this work. Rogowski coil was used to find the AC current, and determine the total power.

The discharge current was measured for the different values of the applied voltage of the DBD system at two values of frequency 8 and 9 kHz with 3 mm dielectric materials and 2 mm distance between electrodes and Epoxy/Al composite dielectric.

Figure 2 shows the wave shape of the voltage applied to the reactor and the corresponding discharge current in the presence of a single epoxy/Al composite dielectric barrier at a 2.0 mm reactor gap between the electrodes.

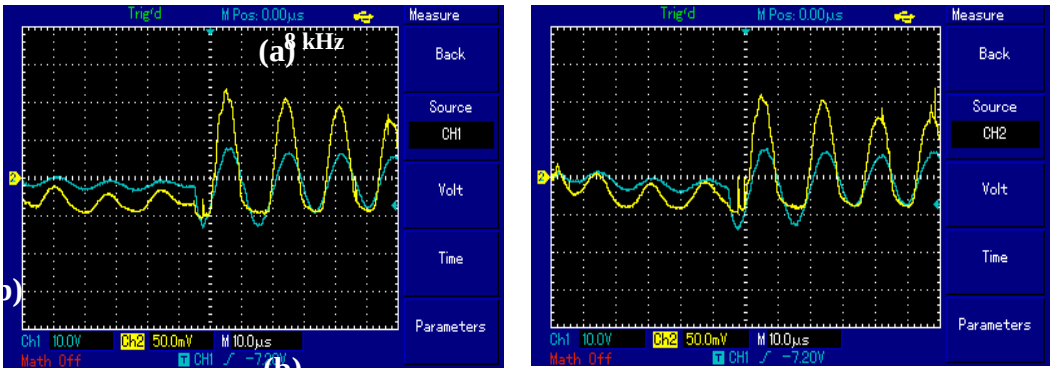

Figure 2: Wave shape of the voltage applied and current at frequency a- 8 kHz and b- 9 kHz for Epoxy/Al composite

The filamentary streamer began in the air gap with random distribution over the entire electrode surface when the A.C. voltage applied to the DBD reactor reached the onset value, as seen in this figure.

The filamentary streamers crossed the air gap and propagated across the epoxy dielectric barrier surface, causing surface charges to accumulate. As a result, the electric field produced by these surface charges was of opposite polarity to the electric field produced by the applied voltage. These streamers that started in the spot point extinguished after a short period, causing streamers to start in another site. The discharge current across a single epoxy dielectric approaches zero when the applied voltage reaches its maximum value, and the streamer's activities cease to exist. The filamentary streamers then restart when the applied voltage reaches the starting value during the following half cycle. It can be shown in Figure 2 that both waveforms have the same behavior.

I-V curves of DBD system at frequency 8 kHz and 9 kHz are shown in Figure 3. It is observed that the discharge current increases linearly with the applied input voltage and also with increasing displacement from center of electrode. This rise is due to the electrons obtaining enough energy to trigger further ionization, resulting in an electron avalanche and the production of a micro discharge inside the DBD system's discharge gap. For each displacement (d), it can be seen that the discharge current rises with the rising of the frequency of the applied voltage. Where at 9 kHz the discharge current increases but applied voltage decreases by comparison at 8 kHz. Optical images were taken for each frequency as shown in Figure 4.

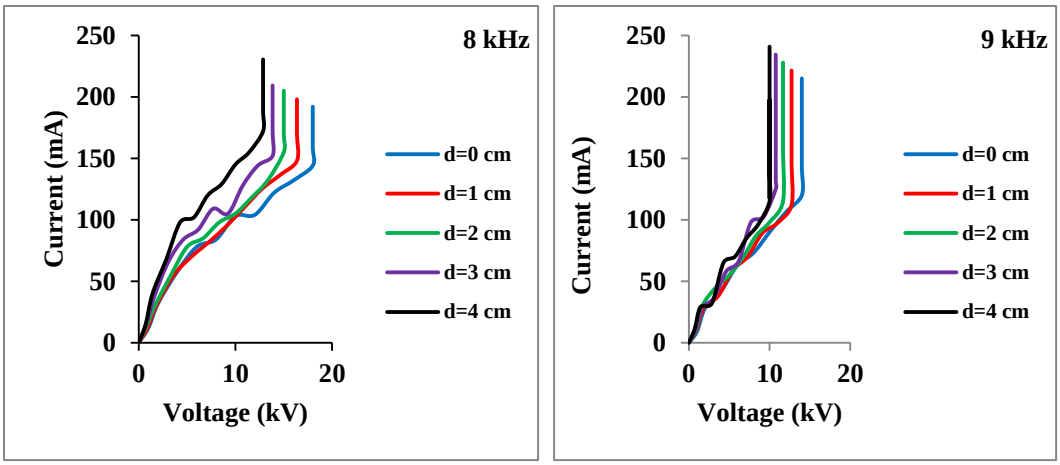

Figure 3: I-V curves of DBD actuator at frequency 8 and 9 kHz at 2 mm reactor gap.

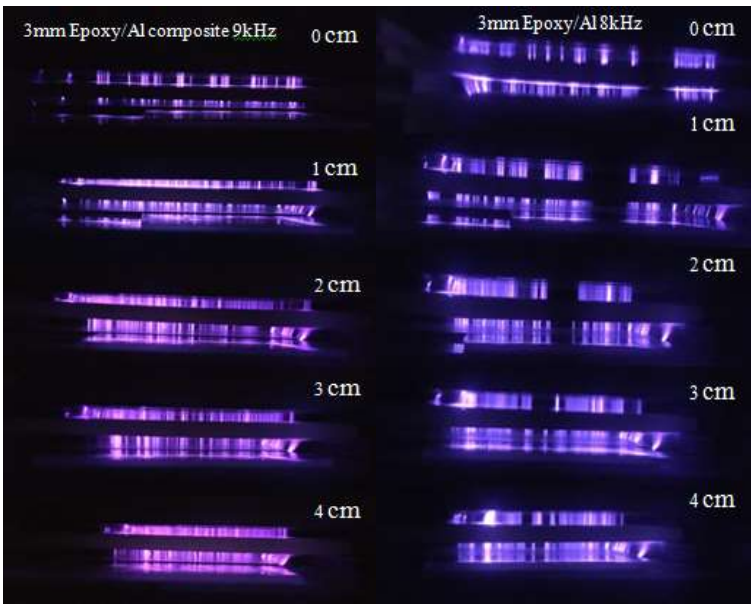

Figure 4: A Photograph of plasma produced between two parallel electrode DBD actuator at frequency 8 kHz and 9 kHz for Epoxy/Al composite dielectric.

4.2. Emission Spectra of surfaced plasma on epoxy/Al composite

The surface plasma spectra for DBD actuator at atmospheric pressure with epoxy/Al composite dielectric with different horizontal distances with applied voltage of up to 20 kV for 8, 9 kHz frequencies are shown in Figures 5 and 6.

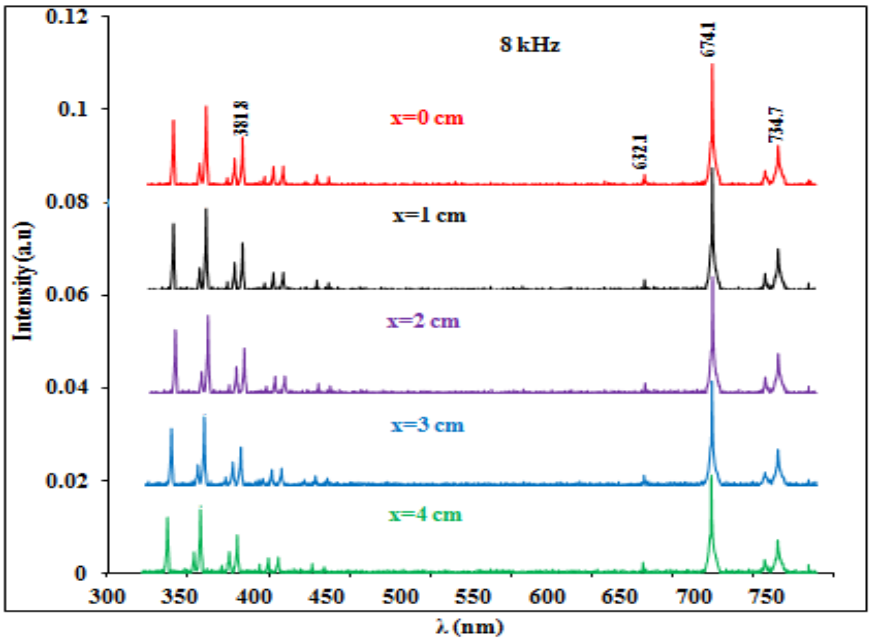

Figure 5: The plasma spectra with different horizontal distance for epoxy/Al composite dielectric at different frequencies 8 kHz.

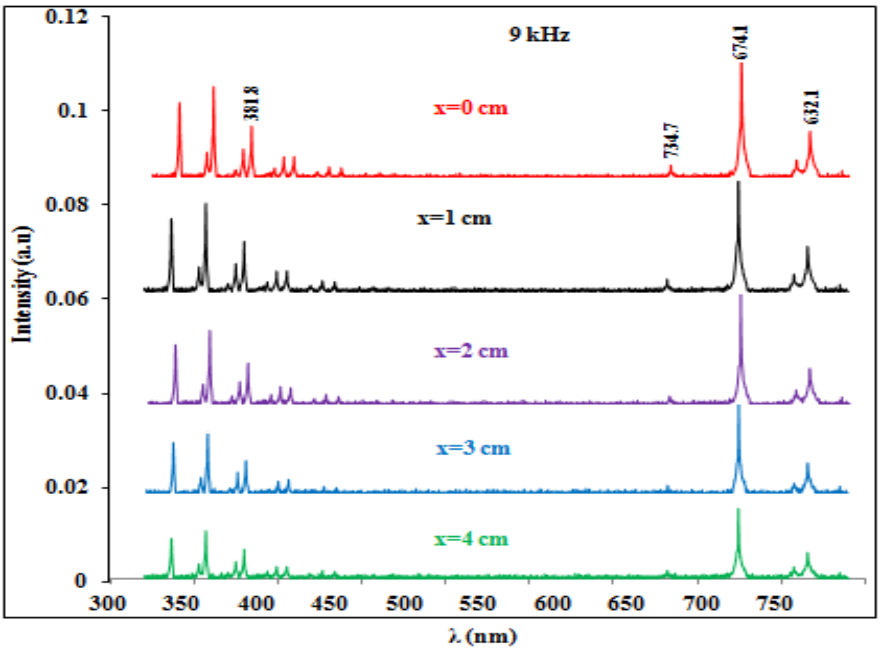

Figure 6: The plasma spectra with different horizontal distance for epoxy/Al composite dielectric at different frequencies 9 kHz.

Many peaks were noted in the wavelength range from (300 to 750) nm. The atomic NI peaks 381.8, 632.1, 674.1 and 734.7 nm are illustrated in Figures (5) and (6). The intensity of the 632.1nm peak decreased with increasing the horizontal distance. The variation of peak intensities for NI at λ= 632.1nm for the two frequencies are shown in Figure 7. It can be seen that the peaks intensities for the 9 kHz are higher than that of the 8 kHz, which is due to an increase in the potential difference between the electrodes that led to an increase in the energy. This result agreed with that of Souza [25]. The spectrum's peak intensity for each frequency reduces with the increase of the horizontal distance i.e. with the decrease of the upper electrode's horizontal surface area. The intensity of emission of plasma-generated

excited species is, of course, dependent on the applied voltage and flow velocity; this fact agrees with reference [26].

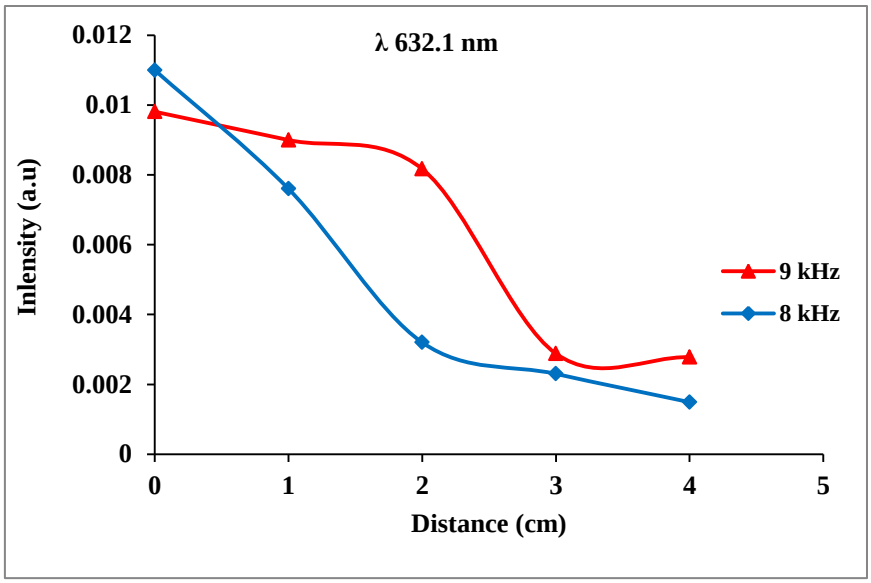

Figure 7: The variation of the maximum line intensities with different horizontal distance for epoxy/Al composite dielectric.

The various excitation and ionization processes that occur in plasma are dependent on the electron temperature (T_e). T_e can be determined when the plasma is supposed to be in LTE and that the population of excited atoms is distributed according to the Boltzmann distribution. The value of T_e was calculated according to Eq. 3 with the required data listed in Table 1. This requires peaks that originated from the same atomic types with data from NIST database. Figures 8 and 9 show the Boltzmann plots, through which the electron temperature was calculated.

Table 1: NI standard lines are used to calculate electron temperature, and their characteristics.

λ (nm)	$A_{ji}\, g_i$	E_i (eV)	E_k (eV)
381.8	3.58E+06	10.67967	13.92588
632.1	7.34E+05	11.99558	13.95634
674.1	6.20E+05	11.8397086	13.67827
734.7	3.33E+05	12.00961	13.6965647

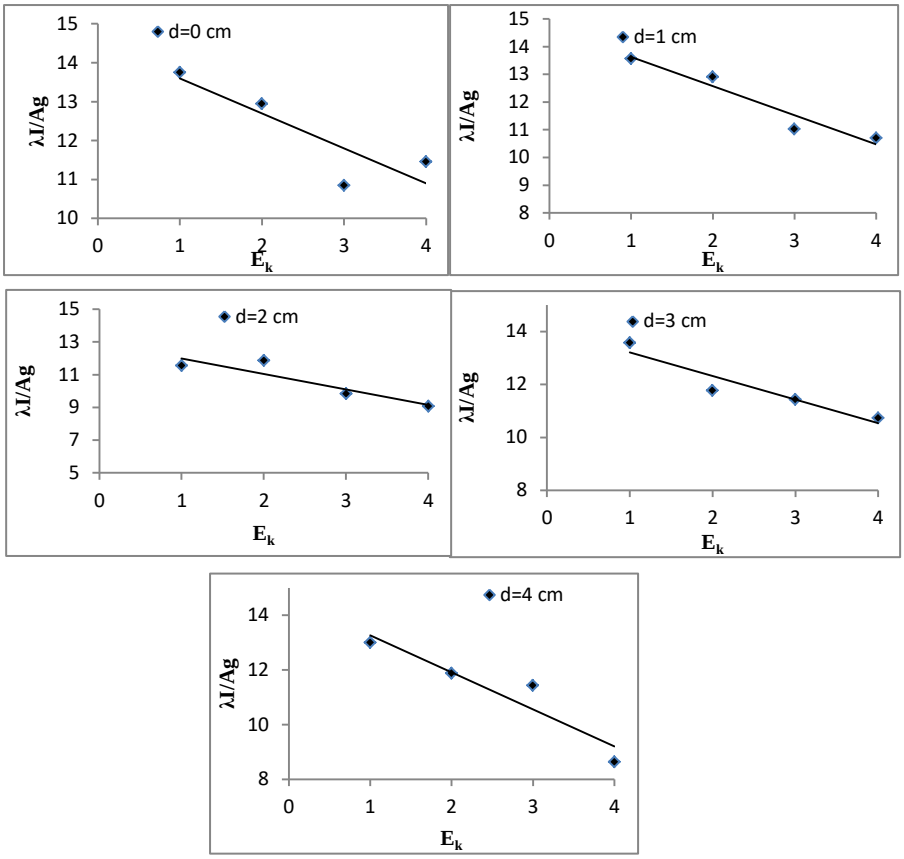

Figure 8: Boltzmann plots of epoxy/Al composite at 8 kHz frequency at different horizontal distances.

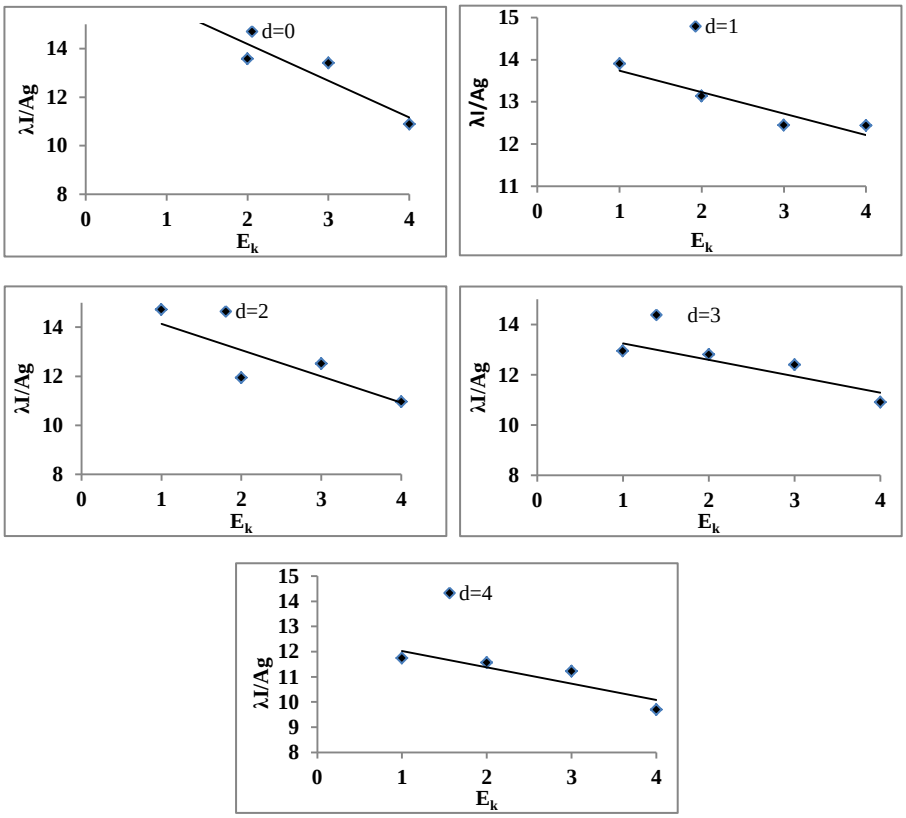

Figure 9: Boltzmann plots of epoxy/Al composite at 9 kHz frequency at different horizontal distances.

The effect of the horizontal distance and frequency on DBD Plasma temperature using the epoxy/Al composite dielectric is illustrated in Figure 10. The electron temperature increase with the increases of the horizontal distance (decrease of the horizontal surface area of the upper electrode) at 8 kHz, and 9 kHz.

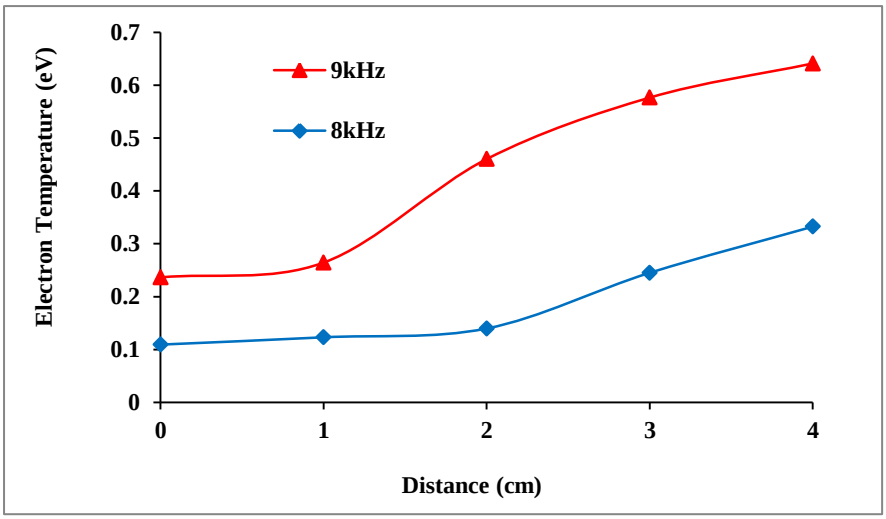

Figure 10: The variation of T_e with the horizontal distance.

This is due to the fact that the electric resistance of the external circuit decreases with the increase in the horizontal distance (decrease of the horizontal surface area), which results in the increase of the discharge voltage across the gap, accordingly, the discharge across the gap is multiplied [27]. An increase in the frequency leads to an increase in the potential difference between the two electrodes, which leads to an increase in the temperature of the electron, as noted from Figure 10. Figure 11 illustrates the Lorentzian fitting which is used to find the full width at the half limit ($\Delta\lambda$) for the 674.3 nm wavelength, which was utilized to calculate the electron density as shown in Figure 12.

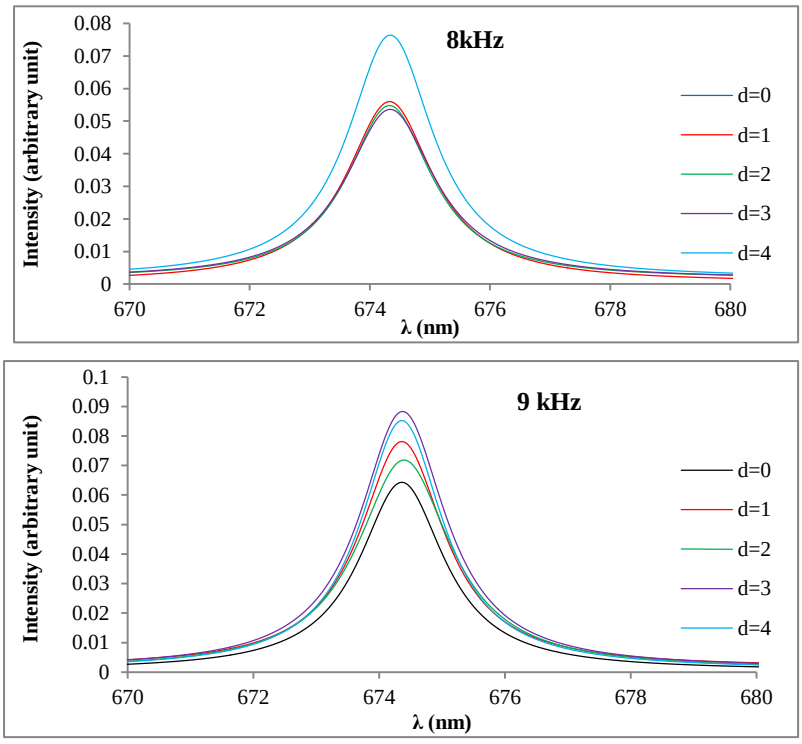

Figure 11: 674.3 nm peaks broadening and Lorentzian fitting at f=8 kHz and 9 kHz

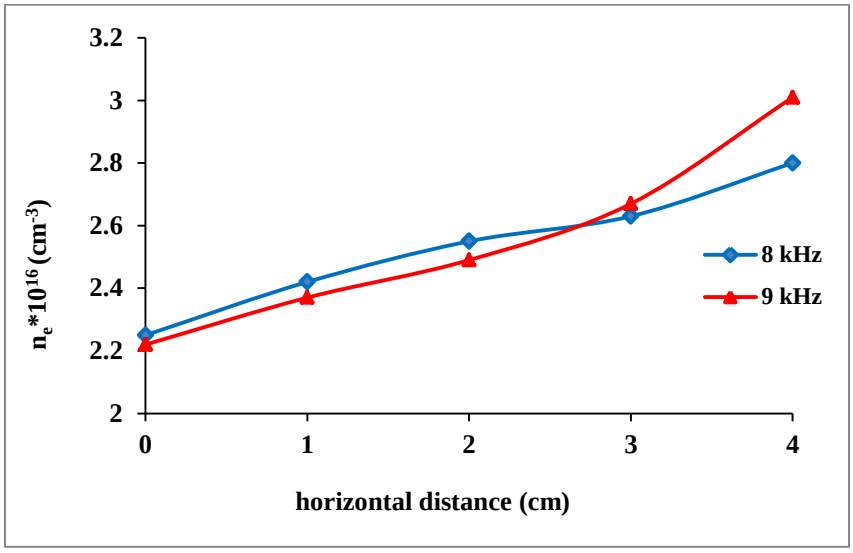

Figure 12: Variation of n_e with horizontal distance at f=8 kHz and 9 kHz.

Using the Stark effect based on the usual broadening values for this line Equation 4. From this equation the electron density can be calculated at various distances utilizing the values (ω_m = 0.155 Å for peak λ=674.3 nm) [28]. It was noted that the decrease in the peak intensity with increasing the horizontal distance means a decrease in the NI species emission in DBD plasma. At 8 kHz frequency, there was a decrease in the intensity which may be due to the saturation of plasma ionization.

The electron density increased with increasing the distance at the high applied voltage due to the ionization stopping in the gas. Using Eq.5, it can be noted that the Debye length (λ_D) varied with the horizontal distance as shown in Figure 13. It turned out that the Debye length decreased with the increase of the distance as a result of the increase in the temperature of the electron. At 9 kHz Debye length increases with the distance.

The change of electron frequency with the horizontal distance is shown in Figure 14. The frequency of the applied voltage has a positive effect on the electron frequency therefore ω_p has a high value at 9 kHz while is constant at 8 kHz as show in Figure 14.

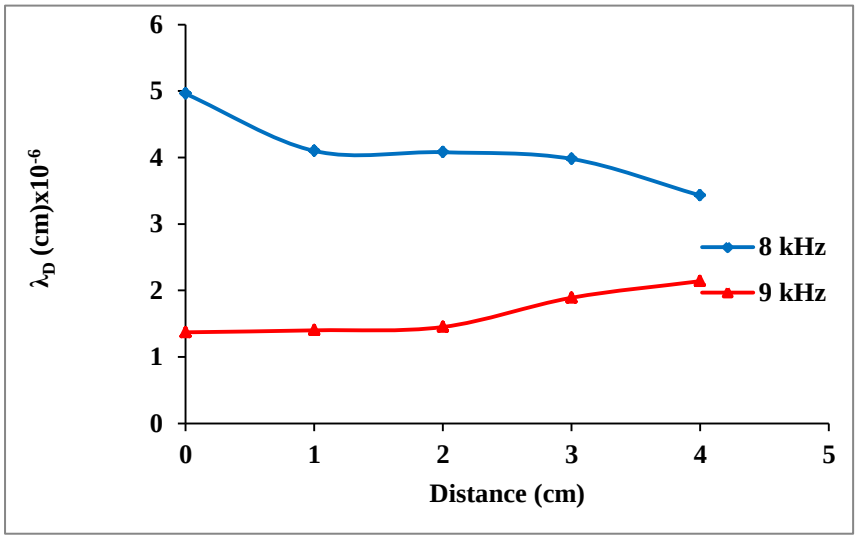

Figure 13: The variation of λ_D with distance or surface area corresponding to the electrodes at f=8 kHz and 9 kHz.

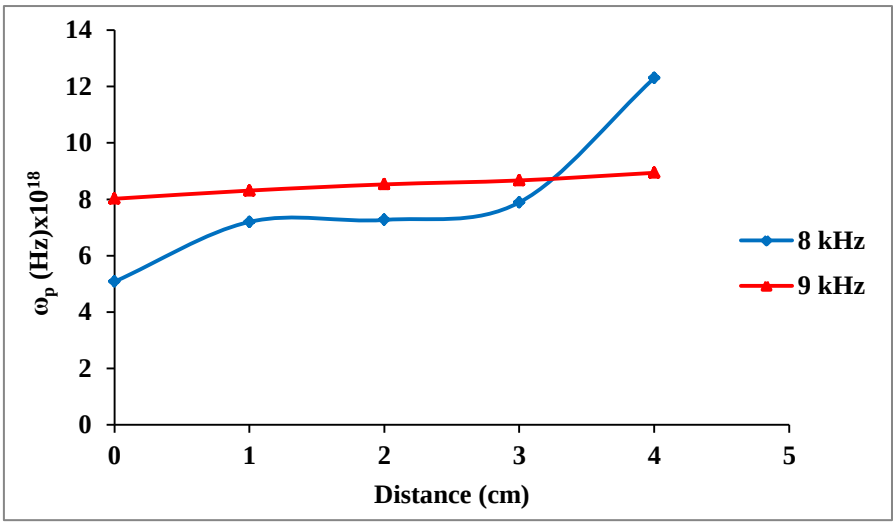

Figure 14: Variation of ω_p with distance or surface area corresponding to the electrodes at f=8 kHz and 9 kHz.

5. Conclusion

The dielectric barrier discharge (DBD) system was successfully designed and constructed using dielectric barrier of epoxy/Al composite. From the results of the work the following points can be concluded:

The filamentary streamer started in the air gap when the voltage applied to the DBD actuator reached the starting value; the number of micro discharges was found to increase with increasing the applied voltage. At atmospheric pressure, the primary spectra lines observed during Epoxy/Al composite dielectric barrier discharge were related to NI excited spectra. When the smallest area was exposited between the electrodes, the highest spectra intensities were observed at 8 kHz and 9 kHz frequencies, the highest intensities were obtained in this parameter. T_e, n_e, and ω_{pe} increased with increasing distance, while the Debye length showed opposite behavior. From the results, the 9 kHz frequency has high effects on the plasma parameters. This is because an increase in frequency leads to an increase in energy and thus an increase in electrical discharge, which increases the values of the plasma parameters.

References

[1] M. Nura, Y. A. Ameliaa, F. Ariantoa, W. Kinandana, I. Zaharb, A. I. Susana and a. J. P. Wibawac, "Dielectric Barrier Discharge Plasma Analysis and Application for Processing Palm oil mill effluent," *Journal Procedia Engin*, vol. 170, pp. 325-331, 2017.

[2] R. Brandenburg, "Corrigendum: Dielectric barrier discharges: progress on plasma sources and on the understanding of regimes and single filaments , Vol. 26, No. (2017), p. 1-29," *Plasma Sources Science and Technology*, vol. 26, pp. 1-29, 2017.

[3] S. Kanazawa, M. Kogoma, T. Moriwaki and a. S. Okazaki, "Stable glow at atmospheric pressure," *J. Phys. D Appl. Phys*, vol. 21, no. 5, p. 838–840, 1988.

[4] F. Massines, A. Rabehi, P. Decomps, R. B. Gadri, P. Segur and a. C. Mayoux, "Experimental and theoretical study of a glow discharge at atmospheric," *JOURNAL OF APPLIED PHYSICS*, vol. 82, no. 6, pp. 2950-2957, 1998.

[5] J. Roth, M. Laroussi and C. Liu, "Experimental generation of a steady-stateglow discharge at atmospheric pressure," *Proc. IEEE Int. Conf. Plasma Sci*, pp. 170-171, 1992.

[6] Cristina Venturini, " Virus inactivation through cold plasma," PhD Thesis, University of Padua, pp. 1-2, 2020.

[7] L. Heping, C. Guoxu, W. Zhibinl and G. N. a. B. Chengyu, "Characteristics of the Large Area Surface Dielectric Barrier Discharge with a Multi-Electrode Configuration," *Journal High Voltage Engineering*, vol. 39, no. 9, pp. 2125-2130, 2013.

[8] M. Schiorlin, C. Paradisi, R. Brandenburg, M. Schmidt, E. Marotta and A. G. a. R. Basner, "Pollutant Degradation in Gas Streams by means of Non-Thermal Plasmas", *Environmental Science*, 2015.

[9] B. Nicholas and a. D.Wilde, "A Model of Surface Dielectric Barrier Discharge Power," *Applied Physics Letters*, vol. 118, no. 15, pp. 1-8, 2021.

[10] M. A. B. Moreira, F. Rodrigues and a. J. Páscoa, "Experimental Study of Dielectric Barrier Discharge Plasma Actuators for Active Flow Control," *KnE Engineering / International Congress on Engineering — Engineering for Evolution*, p. 487–499, 2020.

[11] K. Kostov, R. Y. Honda and L. A. a. M. Kayama, "Characteristics of Dielectric Barrier Discharge Reactor for Material Treatment," *Brazilian Journal of Physics*, vol. 39, no. 2, pp. 322-325, 2009.

[12] U. Kogelschatz, "Dielectric-barrier Discharges: Their History, Discharge Physics, and Industrial Applications," *Plasma Chemistry and Plasma Processing*, vol. 23, no. 1, pp. 1-46, 2002.

[13] E. W. Egli, "Dielectric-Barrier Discharges. Principle and Applications," *Journal De Physique*, vol. 7, no. 4, pp. 47-66, 1997.

[14] J. Hong, Atmospheric Pressure Plasma Chemical Deposition by Using Dielectric Barrier Discharge System , (2013), p. 34-36., Thesis, University of Illinois at Urbana-Champaign, 2013.

[15] H. H. Ley and A. Y. a. R. K. R. Ibrahim, "Analytical Methods in Plasma Diagnostic by Optical Emission Spectroscopy: A Tutorial Review," *Journal of Science and Technology*, vol. 6, no. 1, pp. 49-66, 2014.

[16] I. K. S. Iordanova, "Optical emission spectroscopy diagnostics of inductively-driven plasmas in argon gas at low pressures," *pectrochimica Acta Part B*, vol. 62, pp. 344-356, 2007.

[17] B. M. Ahmed, "Plasma Parameters Generated from Iron Spectral Lines By Using LIBS Technique," *IOP Conf. Series: Materials Science and Engineering*, vol. 928, pp. 1-11, 2020.

[18] M. M. Hossain, *Plasma Technology for Deposition and Surface Modification, Berlin, German: Logos Verlag Berlin GmbH*, 2009.

[19] N. Ohno, M. A. Razzak, H. Ukai and S. T. a. Y. Uesugi, "Validity of Electron Temperature Measurement by Using Boltzmann Plot Method in Radio Frequency Inductive Discharge in the Atmospheric Pressure Range," *Plasma and Fusion*, vol. 1, no. 028, pp. 1-9, 2006.

[20] W. I. Yaseen, A. F. Ahmed and D. A. A.-S. a. F. A.-H. Mutlak, "Development of a high-power LC circuit for generating arc plasma and diagnostic via optical emission spectroscopy," *Journal Applied Physics A*, vol. 128, no. 2, pp. 1-9, 2022.

[21] A. Kramida and Y. R. a. J. Reader, "NIST atomic spectra database," *Natl. Inst. Stand. Technol*, 2014.

[22] A. R. K. H. a. M. A., "Study the Plasma Parameters due to the Different Energies for Laser Produced Lead Oxide Plasma," *Indian Journal of Natural Sciences*, vol. 10, no. 57, pp. 17908-17914, 2019.

[23] A. A.-K. Hussain and K. A. A. a. W. I. Yaseen, "Diagnostics of low-pressure capacitively coupled RF discharge argon plasma," *Iraqi Journal of Physics*, vol. 12, no. 27, pp. 76-82, 2015.

[24] F. E. Chen, *Plasma Physics and Controlled Fusion, New York and London: A Division of Plenum Publishing Corporation*, 1983.

[25] I. A. d. Souza, "Study of the influence of variation in distances between electrodes in spectral DBD plasma excitation," *Mater, Res*, vol. 19, no. 1, pp. 202-206, 2016.

[26] S. B. B. a. M. V. Freamat, "Vibrational spectra of N2: An advanced undergraduate laboratory in atomic and molecular spectroscopy," *J. Phys*, vol. 80, no. 8, pp. 664-669, 2012.

[27] L. H. a. B. Z. P. Liu, "Discharge and Optical Emission Spectrum Characteristics of a Coaxial Dielectric Barrier Discharge Plasma-Assisted Combustion Actuator," *Journal, Spectroscopy*, vol. 2020, 2020.

[28] N. Konjević, A. Lesage and J. R. F. a. W. L. Wiese, "Experimental Stark Widths and Shifts for Spectral Lines of Neutral and Ionized Atoms (a Critical Review of Selected Data for the Period 1989 through 2000)," *J. Phys. Chem. Ref. Data*, vol. 31, no. 3, pp. 819-927, 2002.